Energy Conversion and Management 232 (2021) 113880

Contents lists available at ScienceDirect

Energy Conversion and Management

journal homepage: www.elsevier.com/locate/enconman

An improvement to waste heat recovery in internal combustion engines via combined technologies

D. Di Battista *, F. Fatigati, R. Carapellucci, R. Cipollone

Department of Industrial and Information Engineering and Economics, University of L'Aquila, P.le Ernesto Pontieri, 1 – Monteluco di Roio, 67100 L'Aquila, Italy

ARTICLE INFO

Keywords:
Supercritical carbon dioxide
Energy efficiency
Waste heat recovery

ABSTRACT

Waste heat recovery (WHR) in internal combustion engines (ICEs) is very interesting opportunity for reducing fuel consumption and CO_2 emissions. Among the different heat sources within an ICE, exhaust gases are certainly the most suitable for potential recovery.

The most promising technology is represented by power units based on organic Rankine cycles (ORCs). Unfortunately, their actual efficiency is far from that obtainable using only thermodynamic evaluations: low efficiencies of small-scale machines, strong off-design conditions, and backpressure effect are the main reasons. To improve the conversion efficiency, this paper presents a combined solution, coupling two thermodynamic cycles: Joule-Brayton and Rankine-Hirn ones. The first (top cycle) considers supercritical CO_2 as the working fluid and the second considers an organic fluid (R1233zDe, bottom cycle). The combined recovery unit inherently introduces further complexity, but realizes an overall net efficiency 3–4% higher than that of a single ORC-based recovery unit.

The hot source is represented by the exhaust gas of an IVECO F1C reciprocating engine, considering twelve experimental operating conditions that fully represent its overall behaviour. The combined unit was modelled via a software platform in which the main components of the ORC unit were experimentally validated. The best thermodynamic choices of the top and bottom cycles, as well as their mutual interference, were identified under the condition of maximum power recoverable; this implies an overall optimization of the combined unit considered as an integrated system. Moreover, the components must be handled when off-design conditions (produced by the unavoidable variations of the hot source) occur: insufficient heat transferred to the two working fluids, produced by an over- or under-designed heat exchanger, would prevent the proper operation of the two units, thereby reducing the final mechanical power recovered. To address this critical issue, the three main heat exchangers were designed and sized for a suitable ICE working point, and their behaviour verified to guarantee a suitable maximum temperature of the supercritical CO_2 and full vaporisation of the organic fluid. These two conditions assure the operability of the combined recovery system in a wide range of engine working points and a maximum recovered mechanical power up to 9% with respect to the engine brake one.

1. Introduction

Waste heat recovery (WHR) is one of the most promising opportunities for reducing specific fuel consumption in the industrial and transportation sectors, supporting global targets for energy efficiency and greenhouse gas emission reduction. Global theoretical WHR potential is in the order of 5–15% of the global input energy. The industry sector, in particular, has a theoretical WHR potential of approximately 15% and several technologies are related to the exploitation of this thermal power [1]. These are mainly related to the combined heat and power (CHP) concept, which significantly reduces the primary energy consumption [2,3]. Even cold generation through adsorption chiller can be introduced, when simultaneously cooling capacity is required [4,5], and thermal or cooling storage section cane be introduced requests [6]. Hence, the conversion of residual heat into mechanical/electrical forms is very interesting. Thermodynamic cycles have been proposed to achieve consistent energy recovery, mainly using organic fluids — organic Rankine cycles (ORC) — with very good results for stationary medium and large-scale applications and a low fluctuation range [7–9] in terms of the heat source.

The transportation sector was found to be the largest sector for

* Corresponding author.
E-mail address: davide.dibattista@univaq.it (D. Di Battista).

https://doi.org/10.1016/j.enconman.2021.113880
Received 17 November 2020; Received in revised form 17 November 2020; Accepted 22 January 2021
Available online 11 February 2021
0196-8904/© 2021 Elsevier Ltd. All rights reserved.

Nomenclature

Acronyms	Symbols
BSFC	Brake Specific Fuel Consumption
CHP	Combined Heat and Power
ESC	European Stationary cycle
HRVG	Heat Recovery Vapor Generator
HT-HX	High-Temperature Heat Exchanger
ICE	Internal Combustion Engine
ORC	Organic Rankine Cycle
sCO_2	supercritical CO_2 cycle
WHR	Waste Heat Recovery

Subscripts

A	heat transfer area
Bo	boiling number
Co	Convection number
c_p	specific heat
D_h	hydraulic diameter
f	Fanning factor
h	enthalpy
H	convective heat transfer coefficient
I	irreversibility
k	conductive heat transfer coefficient
m	mass flow rate
P	power
Pr	Prandtl number
Re	Reynold number
s	entropy
T	temperature
t	thickness
v	velocity
x	vapour quality
η	efficiency
ρ	Density
1…9	thermodynamic section
c, comp	compressor
cond	condenser
en	energetic
ex	exergetic
ex1	exhaust gas inlet section
ex2	exhaust gas outlet section
exh	exhaust
is	isentropic
l	liquid
p	pump
ref	reference
sl	saturated liquid
sv	saturated vapor
t, turb	turbine
th	thermal
tot	total (sCO_2 + ORC)
u	useful

recoverable waste heat, with 40–45% of the global theoretical recovery potential [1]; in particular, for heavy-duty vehicles, where lower significant limitations on weight, encumbrances, etc. are experienced [10]. Many technologies are considered to recover energy from exhaust gases: thermoelectric generators are simpler but have low efficiency [11]; turbo-compounding and direct recovery are already applied in medium and heavy-duty vehicles but require proper management, typically via an electric drive [12,13]. ORC units are the most studied but their final energetic and exergetic efficiencies in real operation are definitively low [14,15]. The main reasons for this are:

(a) expander and pump efficiencies — which are conditioned by the size of the machine — are usually realized for large units and are unattainable for applications whose mechanical power is below 10 kW;
(b) ratio between the expansion and compression work decreases when other fluids are considered (with respect to water) and when the maximum temperature of the heat source decreases [16,17];
(c) high temperature of the heat sink, definitively represented by the ambient conditions;
(d) frequent operation at off-design conditions, which reduces the effectiveness of the heat exchangers.
(e) mismatch between the temperature-entropy curves of the heat source and that of the organic working fluid during heat transfer;

A supercritical Rankine-Hirn cycle can address the final point, which limits the recoverable energy [18]. In this way, the "temperature distance" in the T-s plan between the exhaust gas and the working fluid is reduced and so is the irreversibility associated with the heat transfer between the two fluids: the heat exchange efficiency based on the second thermodynamic principle increases and, thus, the specific work of the cycle. To reinforce this concept, the working fluid — usually organic — is substituted with CO_2. The basic thermodynamic cycle can be "trans-critical", when the lower isobaric transformation is achieved under the critical pressure and condensation occurs at this lower pressure, or "supercritical" when the lower pressure is higher than the critical one and, in this case, the Joule-Brayton cycle is used for reference [19]. For both a supercritical and trans-critical thermodynamic cycle, the T-s behaviour of the isobaric curves shows a very high specific heat near the critical point [20]. The heating of the supercritical CO_2 can proceed very close to the exhaust gas cooling owing a very limited pinch difference [21], which reduces the heat transfer irreversibilities and increases the cycle area (so, the specific work of the cycle). It is established that a CO_2 supercritical/trans-critical cycle has higher efficiency than an ORC cycle [22]; in particular, if the organic working fluid selection is limited to non-flammable and non-toxic fluids [23]. The thermal efficiency (based on the first thermodynamic principle) of the cycle can be significantly improved by introducing an internal regenerator that recovers part of the thermal power at the expander outlet to heat the compressor outlet gas (in the supercritical cycle) or the pump outlet liquid (in the trans-critical cycle) [24]. The main drawback of this internal recovery is related to the great specific heat difference between the two isobaric curves (i.e., the CO2 exiting the expander to be cooled and the same CO_2 fluid that exits the pump or the compressor to be heated). This leads to significant exergetic losses inside the regenerator [25]. Moreover, this regeneration stage prevents any further low-temperature heat recovery and possible thermodynamic cycle cascade.

The integration of supercritical/trans-critical CO_2 cycles with other thermodynamic cycles (i.e., ORC), can be realized in parallel or cascade configurations (Fig. 1, [26]).

In the first case, CO_2 and ORC share the same upper thermal source but with different temperatures and without reaching to exploit the best waste heat [27]. Therefore, a recompressed cycle has been proposed, as well as a dual-expansion cycle [28].

In the second case, the ORC has the role of recovering the residual CO_2 heat. Hence, the CO_2 cycle recovers energy from the upper thermal source, releasing heat at a lower temperature, which, in turn, acts as an upper thermal source for an ORC unit; i.e., the supercritical CO_2 cycle is placed between the thermal source to be recovered and the ORC

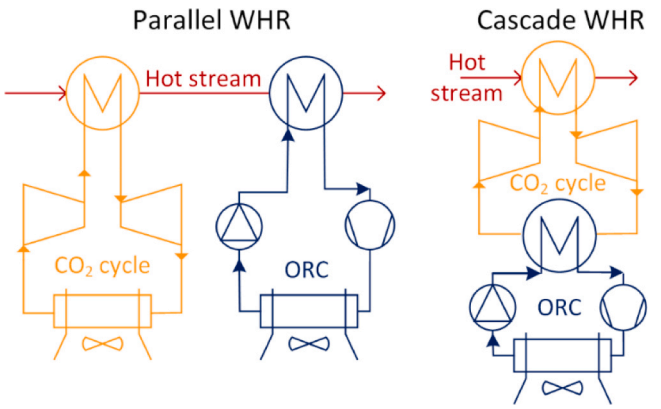

Fig. 1. parallel and cascade configurations of CO_2/ORC waste heat recovery cycles.

thermodynamic cycle.

The specific WHR from the exhaust gas in the ICE has been the subject of a wide range of recent studies exploiting several aspects concerning the fluid choice [29,30], operating conditions [31,32], technology of the components [33], interferences with the engine [34,35] and the vehicle [36,37], control needs [38], and cost and weight of the recovery unit [39,40]. Unfortunately, despite the invested effort, overall net efficiencies greater than 4% are difficult to achieve. In long-haul applications, such as freight/passenger transportation, a more effective recovery would participate in the need to reduce the fuel cost, which is more than 20% of the generalised transportation cost in Europe [41], and other substances (e.g., urea used for the SCR NOx abatement) whose consumption is proportional to fuel use.

Currently, the baseline value of CO_2 emissions for long-hauling vehicles is 56.5 g/tkm [42] (referred to as the unit of distance in kilometres and weight transported in tonnes), considering the group vehicles with the highest fleet share. The EU regulation imposes two time constraints for CO_2 emission reduction: a relative 15% reduction for the reporting periods 2025 – 2029 and 30% from 2030 onwards [43]. Therefore, a significant effort is required to fulfil a challenging target in the next decade.

Considering the limitations for the WHR in ICE, particularly concerning exhaust gases, an urgent need for a breakthrough technology is required, even though it will be characterized by an additional complexity and cost of the recovery unit. Fortunately, long-haul vehicles do not suffer from frequent transient engine behaviour, but they are managed for medium/long periods and distance travelled. Therefore, an off-design analysis that considers the behaviour of the most important components cannot be neglected.

This paper discusses a more complex recovery unit where two thermodynamic cycles are realized and the second is fully bottomed to the first one. The result is a combined recovery unit that significantly increases the recovered mechanical power and reduces fuel use and CO_2 emissions.

In the proposed combined recovery system, CO_2 performs a Joule-Brayton cycle, with the exhaust gases of the engine as the thermal source. The thermal power to be reversed at a lower temperature is recovered in a heat recovery vapour generator, where an organic fluid is economized, vaporized, and superheated, performing a Hirn cycle (a superheated Rankine cycle). R1233zDe is chosen as the working fluid, since it is considered the most suitable fluid replacement for the widely studied R245fa [44,45], which has a high global warming potential despite its wide consideration in the literature. Considering that the unit will operate on board, the lower temperature source for the Hirn cycle is the environmental air considered within the 40–50 °C range, a value very close to a real operation and higher than the values usually referred to when the unit operates in a lab.

The analysis is completed with an off-design assessment of the performance of the heat exchangers involved in the system. In this study, the heat exchangers are sized for a specific engine working point, choosing among the ESC13 mode homologations. Their performances are evaluated when the engine is operated at the other points of the ESC 13-modes cycle, sweeping a wide operating region of the engine. The simulations benefitted from the wide experimental activity the authors had previously conducted [15,46,47] on an ORC-based power unit bottomed to an ICE on a test bench. In this way, the combined recovery unit proposed is tailored to an on-the-road transportation application: data from the real engine performed on representative working points are used to characterize the upper thermal source and on-board operating conditions for cold sink are considered. The results is a combined small-scale waste heat recovery unit, which is particularly challenging and not so referenced in literature. Moreover, experimental performances of the machines (expander and pumps) for the ORC based power unit are introduced to make results more realistic for the specific sector. The combined recovery unit is affected by a significant off-design behavior due to the temperature and mass flow rate variations of the exhaust gas. In order to get closer to the real achievable recovery, an off-design analysis of the heat exchangers completes the study. A definitive comparison of the combined CO_2 supercritical and simple ORC system has finally been assessed, opening the way to construct a prototype.

2. Materials and methods

The analyses started from the availability of experimental data of an internal combustion engine used for light and heavy-duty vehicles. The data characterises the thermal source, considered an upper thermal source for energy recovery by a supercritical CO_2 cycle coupled to the ORC cycle. Therefore, a thermodynamic analysis was performed to assess the recoverable energy. Then, the off-design behaviour of the heat exchangers was introduced to evaluate the performance of the entire plant during operation, bottomed to the ICE. Further experimental data were taken from a dedicated test bench on ORC bottomed to the ICE to characterize the pump and expander efficiencies in realistic conditions. The experimental campaign, moreover, is needed to characterize the range operability of the combined recovery unit proposed and to tailor its size and that one of its components. Fig. 2 shows a simplified flow chart of the methodology used.

2.1. Experimental campaign on ICE

The waste heat to be recovered by the proposed system is represented by the exhaust gases of an IVECO F1C turbocharged diesel engine used in the transportation sector. In particular, its application in heavy-duty vehicles has been considered. The engine is located on the ICE lab test bench, at the University of L'Aquila, and was fully equipped to assess the exhaust heat reversed to the environment through the flue gases. ESC13 mode working points have been considered as they are the reference procedure for the homologation of heavy-duty vehicles, imposing engine revolution speed and brake load. All the relevant quantities have been measured; in particular, the intake air mass flow rate is measured at the engine inlet, via a hot flow meter, and a fuel balance measures the fuel rate, allowing calculation of the exhaust mass flow rate. The exhaust temperature was measured using a K-type thermocouple. The temperature was measured downstream of the aftertreatment devices, where a possible recovery section can be applied without modifying the emission abatement efficiency. Table 1 summarizes the data used as input for the proposed recovery system and the uncertainties of the quantities monitored.

2.2. Experimental campaign on ORC

The proposed thermodynamic model also benefited from a wide experimental campaign realized on the ORC test bench [15,46,47]. The

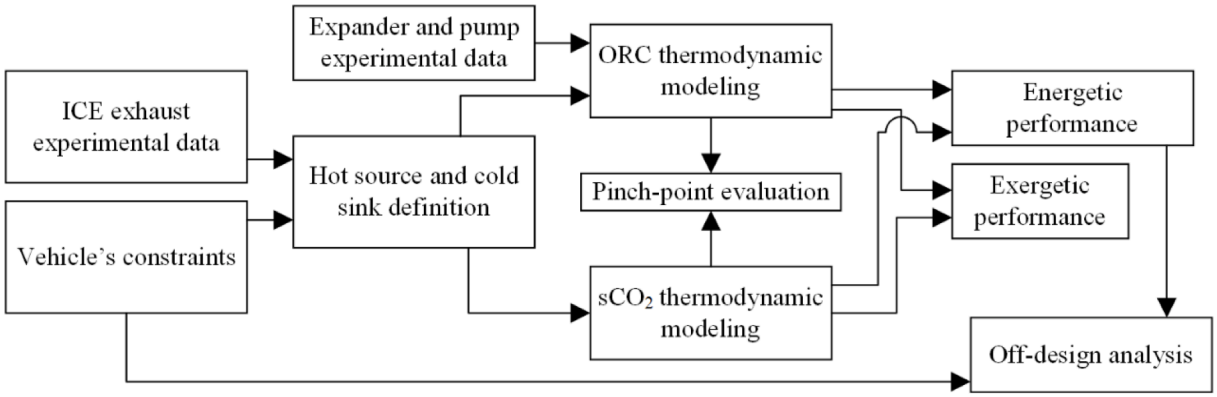

Fig. 2. flow chart of the methodology used.

Table 1
IVECO F1C turbocharged engine testing data.

ESC#	EngineSpeed [RPM]	EngineTorque [Nm]	Load %	T_{ex1} [°C]	Air massflow rate [kg/s]	BSFC[g/kWh]
2	2175	400	100	431.6	0.118	199.2
3	2750	200	50	374.1	0.111	216.6
4	2750	300	75	421.5	0.133	207.8
5	2175	200	50	335.2	0.067	225.5
6	2175	300	75	377.6	0.088	211.9
8	2750	400	100	486.1	0.151	207.7
10	3325	365	100	503.5	0.174	224.1
12	3325	274	75	479.0	0.154	216.7
13	3325	183	50	370.0	0.132	224.1
uncertainty	±1 RPM	± 1%	–	±2.2 °C	±3%	±0.5%

upper thermal source is represented by the exhaust gases of the same turbocharged diesel engine.

Here, the data are rearranged to select the optimal technologically achievable range of efficiencies.

In particular, the pump is volumetric type: it has been fully characterized, both experimentally and numerically, with the possibility of changing its revolution speed to match the mass flow rate required to vaporise the fluid in the heat recovery vapour generator (HRVG). In other word, the pump has been tested in different changing the revolution speed and varying the thermodynamic conditions of the upper thermal source, so changing the pressure head of the circuit served by the pump. Temperature and pressures across the pump are measured and its efficiency evaluated [48]. Fig. 3 shows the results, where an isentropic efficiency of the pump above 80% can be obtained but a more reasonable average value of 70% has been experienced and is considered in this work. With this value, a wider mass flow rate range is accounted for, thus considering the eventual off-design conditions.

The expander in the ORC section is one of the most delicate components and, therefore, its behaviour should be properly evaluated. A scroll-type machine was considered, which was tested by the authors thanks to a dedicated test bench where mass flow rate, temperatures and pressures are measured with an overall average uncertainty of 5% [47]. Its adiabatic efficiency can be evaluated according to a procedure derived from an experimental review of several similar expanders [49]. This is summarized in Fig. 4, exhibiting an efficiency ranging from 0.6 to 0.8 for suitable operating range. Therefore, a mean value of 70% was considered in this work. In addition, this datum allows to consider an average value that applies to a wide mass flow rate range. When the expansion ratio β is greater than 11, the value underestimates the real expander performance while for lower expansion ratios it still ensures a wider range of validity; e.g., for $\beta = 10$, the underestimation applies until 0.25 kg/s while for $\beta = 8$ the underestimation applies until 0.15 kg/s. The decreasing trend of the isentropic efficiency with working fluid mass flow rate observed in Fig. 4 is the result of the trade-off between volumetric and mechanical efficiency. In particular, Fig. 5 shows the

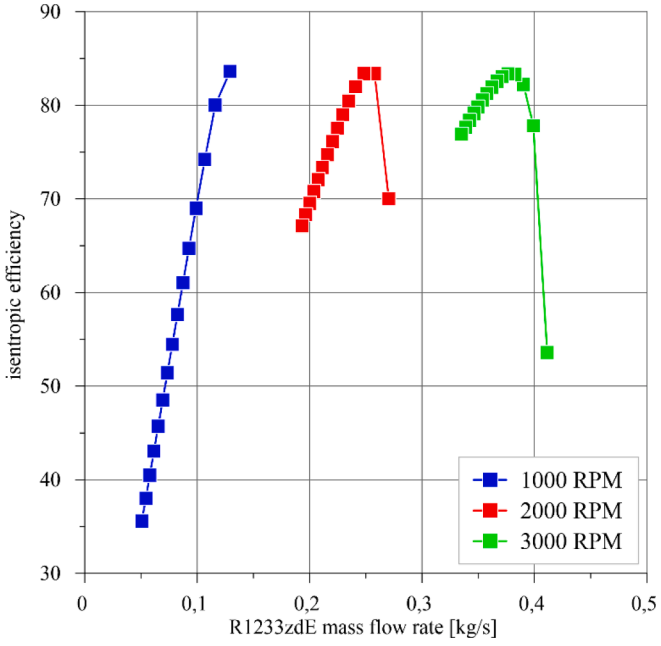

Fig. 3. ORC pump efficiencies [%].

volumetric efficiency, calculated as the ratio between the real and theoretical mass flow rate of a volumetric expander: as the mass flow rate increases, the volumetric efficiency approaches the ideal value equal to 1. Conversely, Fig. 6 shows the lumped mechanical efficiency of the machine, which accounts for the mechanical losses and the indicated efficiency related to heat losses during expansion transformation.

Concerning the machine efficiencies of the supercritical CO_2 cycle, much less knowledge is available in the literature, specifically

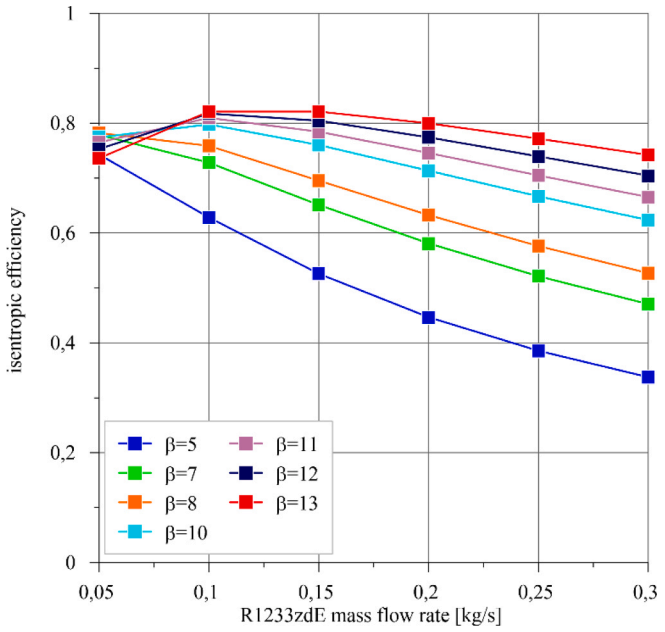

Fig. 4. experimental efficiency data for a scroll expander.

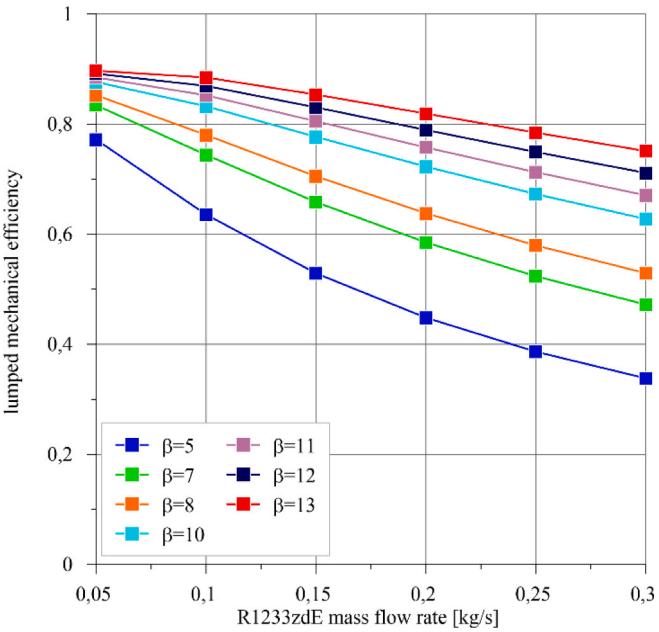

Fig. 6. lumped mechanical efficiency of scroll expander.

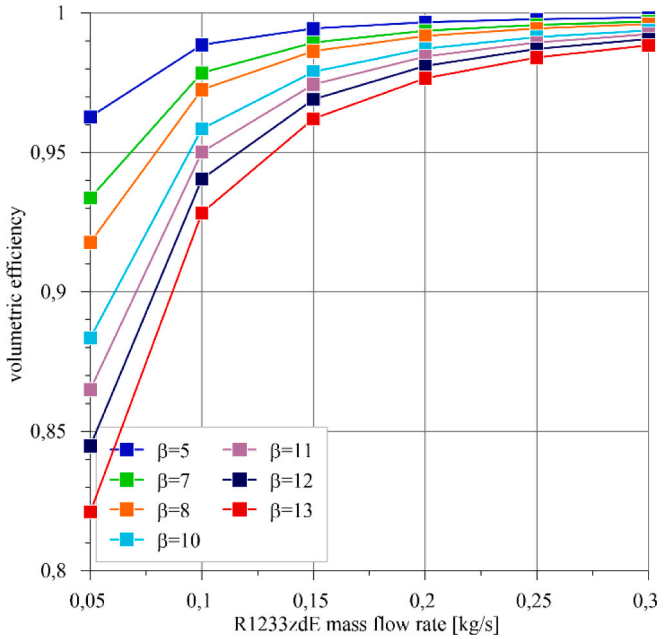

Fig. 5. volumetric efficiency of scroll expander.

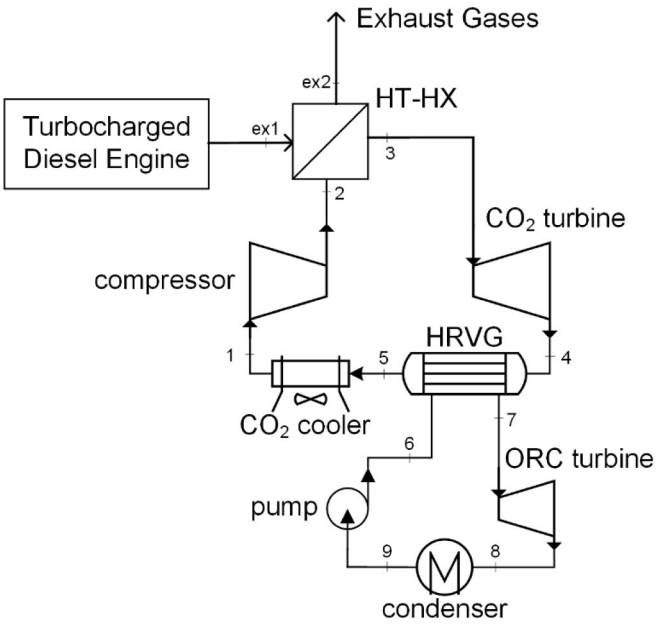

Fig. 7. layout of the proposed combined supercritical CO_2 and ORC recovery system.

concerning expanders and compressors in the range of a few kilowatts. The expected values in this power range are 2 – 6 kW for the compressor and a rated value of 10 kW for the turbine. Hence, an average efficiency of 70% was chosen.

2.3. Thermodynamic modelling

The proposed recovery system is illustrated in Fig. 7. The thermal energy of the exhaust gas is recovered in the high-temperature heat exchanger (HT-HX), where the supercritical CO_2 at high pressure is heated from Section 2 to Section 3. The CO_2 performs a closed Brayton cycle: it is compressed and heated, then expanded in a turbine from Section 3 to Section 4. The heat to be exchanged in the lower isobaric transformation is partially used as the upper thermal source for an ORC unit. Therefore, from Section 4 to Section 5, the CO_2 exchanges its thermal power in the HRVG and, finally, it is cooled to section 1 in the CO_2 gas cooler to reach a suitable temperature in the compression inlet section. This heat exchanger is cooled by environmental air, eventually assisted by a fan. The ORC unit, on the other hand, performs a Hirn cycle. R1233zDe has been considered as a working fluid as it is one of the most suitable candidates owing to its thermodynamic performance and low environmental impact.

In Fig. 8, a T-s diagram of the combined supercritical CO_2 and ORC cycle is presented, considering the data of the ESC#4 working point. This datum is representative of the most frequent operating condition of the thermal engine, i.e., a light-duty mode of operation. This is particularly valid when a heavy-duty mode is considered. Irrespective, the gas temperature is quite high (420 °C) to fulfil the recovery units.

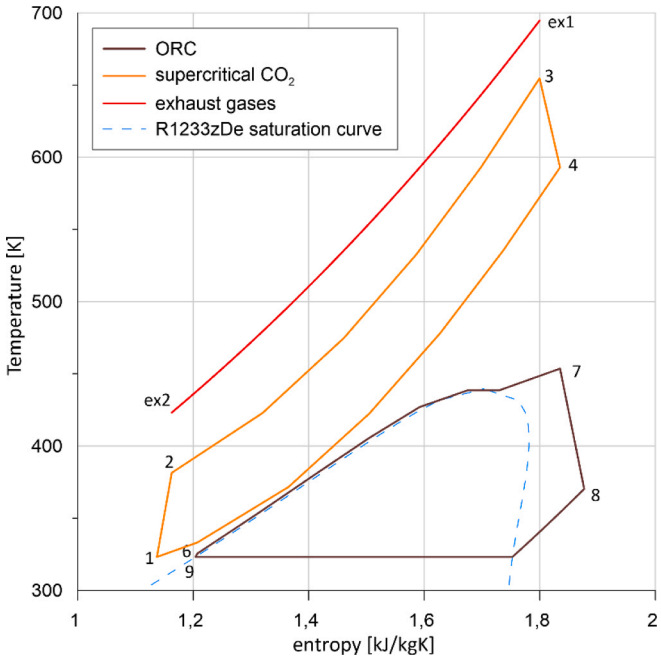

Fig. 8. T-s diagram of the recovery system (1 kg of R1233zDe has been considered as reference mass for the x-axis).

The CO_2 Joule-Brayton cycle is positioned between the exhaust gas T-s diagram and the ORC on the T-s plan providing additional recovered work and a reduction in the exergy losses that would have been present if the top cycle was not introduced. To increase recovery, the T-s plan of the ORC considers a maximum pressure that is close to the critical one one; lower pressures would decrease the power recovered owing to the lower specific work of the cycle and no compensation for the corresponding mass flow rate. It is also evident that the large regeneration, which would be possible for the sCO_2 cycle constituting the majority of the 2–3 heating stage, could be achieved using the high enthalpy of the CO2 at the expander exit. Unfortunately, this potentiality cannot be used to prevent the possibility of feeding the ORC and work recovery from the exhaust gases.

To evaluate the performance of the recovery system on the test turbocharged engine, a thermodynamic model was used and applied to the working points of Table 1, aiming to determine the highest recoverable power [50]. The main equations are summarized as follows: considering the measured temperature of the exhaust gases where the exhaust mass flow rate is the sum of the engine intake air and consumed fuel (Table 1), the thermal power exchanged in the HT-HX was evaluated according to:

$$P_{exh} = m_{exh} c_{p,exh} (T_{ex1} - T_{ex2}) \tag{1}$$

The carbon dioxide mass flow rate that runs in the supercritical section can be calculated by the energy balance of the HT-HX:

$$m_{CO2} = \frac{P_{exh}}{c_{p,exh}(T_{ex1} - T_{ex2})} \tag{2}$$

The thermodynamic assessment of the supercritical CO_2 cycle was performed according to:

$$\begin{aligned} P_{u,CO_2} &= m_{CO_2}[(h_3 - h_4) - (h_2 - h_1)] \\ &= m_{CO_2}[\eta_{t,CO_2}(h_3 - h_{4,is}) - (h_2 - h_{1,is})/\eta_{c,CO_2}] \end{aligned} \tag{3}$$

The heat exchanged in the HRVG is calculated according to:

$$P_{HRVG} = m_{CO_2}(h_4 - h_5) \tag{4}$$

The thermal power to be exchanged to restore the compressor inlet temperature is calculated according to:

$$P_{cooler} = m_{CO_2}(h_5 - h_1) \tag{5}$$

In the ORC section, the mass flow rate of the organic working fluid can be calculated according to:

$$m_{ORC} = \frac{P_{HRVG}}{(h_7 - h_6)} \tag{6}$$

Hence, the useful power of the ORC section is calculated according to:

$$\begin{aligned} P_{u,ORC} &= m_{ORC}[(h_7 - h_8) - (h_6 - h_9)] \\ &= m_{ORC}[\eta_{t,ORC}(h_7 - h_{8,is}) - (h_6 - h_9)/\eta_{p,ORC}] \end{aligned} \tag{7}$$

Finally, the energetic efficiency of the combined recovery system is calculated according to:

$$\eta_{en} = \frac{P_{tot}}{P_{exh}} = \frac{P_{u,CO_2} + P_{u,ORC}}{P_{exh}} \tag{8}$$

The main parameters of the model are summarized in Table 2. The machine efficiency benefits from experimental data, as described in the previous section; 0.7 is in the range of the experienced value and it can be considered as a safety value as the measured value is often higher than this. The lower CO_2 operating temperature should be very close to the critical point to maximize the power output [52]: 50 °C has been chosen, considering the heat sink at 40 °C in mobile applications. In the same low-pressure transformation, the pinch point is chosen as 5 °C, which can be obtained with current heat exchange technology [53]. The maximum CO_2 temperature is chosen as 400 °C, according to known experimental facilities [54] and the evaporating pressure is very close to the critical pressure; no significant benefits are related to supercritical ORC but more operational complications are produced. The ORC CO_2 maximum temperature is limited by the degradation temperature of the working fluid (R1233zdE, [51]) and is equal to 180 °C. As stated, the lower temperature sink is definitively the environmental air as the condenser is a heat exchanger placed in the front end of the vehicle [10], as well as the CO_2 cooler; therefore, the condensation temperature of the ORC is equal to 50 °C.

The model can iteratively solve the energy balance in each section and, in particular, evaluate the minimum temperature difference among fluids in heat exchangers. The model is completed with an exergetic evaluation, calculating the irreversibilities of each component according to Eq. (9). The irreversibilities are calculated as the difference between the inlet and outlet exergy, except for the completely dissipative processes: i.e., the exhaust gas at stack (final outlet section, I_{stack}), condensation $I_{cond,ORC}$, and CO_2 cooling I_{cooler}. The main contributions of these values are related to physical exergy. In particular, considering the exhaust gases, their chemical exergy (related to their different composition from the air) can be neglected as the composition does not change during heat transfer or at stack. Therefore, the irreversibility rate related to the high-temperature heat exchanger (I_{HX-HT}) is calculated considering the exergy associated with the cooling of the exhaust gases down to T_{ex2} and the exergy absorbed by the carbon dioxide at high pressure. In the HRVG, the irreversibility is simultaneously calculated as the difference between the exergy of the hot and cold fluid.

Table 2
model parameters.

Final exhaust gas temperature T_{ex2}	150 °C
Lower CO_2 temperature T_1	50 °C
Maximum CO_2 operating temperature	400 °C
The minimum pinch point difference between CO_2 and organic fluid	5 °C
Expanders isentropic efficiency	0.70
Compressor isentropic efficiency	0.70
Pump isentropic efficiency	0.70
ORC maximum temperature T_7	180 °C
ORC condensation temperature T_9	50 °C

In machinery, exergy is associated with an enthalpy drop or increase and the mechanical power produced or absorbed by each machine ($I_{turb,CO2}$, $I_{turb,ORC}$, $I_{comp,CO2}$, $I_{pump,ORC}$).

$$\begin{cases} I_{HT-HX} = m_{exh}\left[c_{p,exh}(T_{ex1}-T_{ex2}) - T_{ref}(s_{ex1}-s_{ex2})\right] - m_{CO_2}\left[(h_3-h_2) - T_{ref}(s_3-s_2)\right] \\ I_{stack} = m_{exh}\left[c_{p,exh}(T_{ex2}-T_{ref}) - T_{ref}\left(s_{ex2}-s_{ref}\right)\right] \\ I_{turb,CO_2} = m_{CO_2}\left[(h_3-h_4) - T_{ref}(s_3-s_4)\right] - P_{turb,CO_2} \\ I_{comp,CO_2} = P_{comp,CO_2} - m_{CO_2}\left[(h_2-h_1) - T_{ref}(s_2-s_1)\right] \\ I_{HRVG} = m_{CO_2}\left[(h_4-h_5) - T_{ref}(s_4-s_5)\right] - m_{ORC}\left[(h_7-h_6) - T_{ref}(s_7-s_6)\right] \\ I_{cooler} = m_{CO_2}\left[(h_5-h_1) - T_{ref}(s_5-s_1)\right] \\ I_{turb,ORC} = m_{ORC}\left[(h_7-h_8) - T_{ref}(s_7-s_8)\right] - P_{turb,ORC} \\ I_{pump,ORC} = P_{pump,ORC} - m_{ORC}\left[(h_6-h_9) - T_{ref}(s_6-s_9)\right] \\ I_{cond,ORC} = m_{ORC}\left[(h_8-h_9) - T_{ref}(s_8-s_9)\right] \end{cases} \quad (9)$$

The final exergetic efficiency of the combined recovery unit was evaluated according to:

$$\eta_{ex} = \frac{P_{u,CO_2} + P_{u,ORC}}{m_{exh}\left[c_{p,exh}(T_{ex1}-T_{ref}) - T_{ref}\left(s_{ex1}-s_{ref}\right)\right]} \quad (10)$$

2.4. Validation

The model presented has been compared to data from recent literature. It has been applied to the specific layout of the supercritical CO_2 and ORC combined cycle; the supercritical CO_2 recompression Brayton cycle has been reproduced, considering the same machines efficiencies from the reference literature [24,55]. The main resulting parameters have been used for comparison; the output power and exergy efficiency show a very good agreement, as presented in Table 3. Moreover, the minimum temperature difference in the HRVG has been evaluated and compared to that of the two references, having an equal value. This ensures that the heat transfer curves of the current and two reference models overlap.

It is evident that the overall developed model matches the data reported in [24] and [55]; the values are substantially similar and this fully justifies the model's subsequent use as a virtual platform for deeper analyses and development of a real unit.

2.5. Off-design modelling

A very interesting issue is represented by the off-design behaviour of the three major heat exchangers involved in the recovery system. In the transportation sector, one of the main issues related to waste heat recovery from the exhaust gas is the off-design conditions occurring during real operation, considering the significant variations of the duty cycle of the engine in a vehicle. The most important variations are related to the mass flow rate and temperature of the exhaust gases, which affect the behaviour of the HT-HX. Performances of the HRVG and CO_2 cooler, on the other hand, are mainly affected by the CO_2 and organic fluid mass flow rates. These two values can indeed be regulated by the flow control of the compressor and pump to match the thermal powers available in the cascade. The condenser is usually oversized and often a small receiver is placed downstream (section 9 of Figs. 6 and 7) to guarantee the complete condensation of the fluid in each working condition. Therefore, it does not suffer from off-design conditions. Moreover, the off-design of the four machines (compressor and expander of the Joule-Brayton cycle and pump and expander of the ORC-unit) can be preliminarily neglected because they are volumetric and their main advantage, with respect to dynamic machines, is the capability to accept large variations in mass flow rates and thermodynamic conditions [47,56].

Table 3
validation results of the model.

Parameter	Present model	Ref. [24]	Ref. [55]
CO_2 turbine power [MW]	417.9	418.0	418.0
ORC turbine power [MW]	23.5	23.4	23.3
Net power output [MW]	260.7	261.0	261.0
Exergy efficiency [%]	60.2	60.1	60.1
Minimum temperature differencein HRVG [°C]	3.0	3.0	3.0

The off-design modelling of heat exchangers has been one-dimensionally developed, considering the energy, momentum, and energy equations [57]. In particular, each heat exchanger was modelled in a counterflow, dividing the passages of the fluids into finite elementary equivalent ducts, where the thermal energy rating is performed according to the ε-NTU methodology [58]. In each elementary piece of the heat exchanger, the two fluids involved (hot and cold) are grouped on the two sides and the thermal power exchanged P_{th} can be calculated according to:

$$P_{th} = \left(H_{hot} + \frac{k_{wall}}{t_{wall}} + H_{cold}\right)\cdot A\cdot \Delta T_{hot-cold} \quad (11)$$

The heat exchange area A was initially determined for a specific working point (ESC#4 point, Table 1).

The contribution related to t_{wall} and k_{wall} (thickness and thermal conductivity of the exchanger walls) can usually be neglected when compared to forced convective coefficients (H). During the economization and superheating of the organic fluid, the heat transfer coefficient H is calculated according to the Colburn analogy:

$$H = 0.5\cdot f\cdot \rho\cdot v\cdot c_p\cdot Pr^{-2/3} \quad (12)$$

where the Fanning friction factor f is calculated considering turbulent flow, according to:

$$f = \frac{0.08}{\mathrm{Re}^{0.25}} \quad (13)$$

For the evaporation of the organic fluid (two-phase flow), Kandlikar's heat transfer coefficient has been used:

$$H = \left(1.1837\mathrm{Co}^{-0.3} + 225.55\mathrm{Bo}^{0.7}\right)(1-x)^{0.003} H_l \quad (14)$$

where H_l is the heat transfer coefficient referred to the saturation liquid phase, evaluated according to the Dittus-Boelter relation:

$$H = 0.0243\mathrm{Re}^{0.8} Pr^{n}\frac{k_{fluid}}{D_h} \quad (15)$$

The convection number Co and boiling number Bo in Eq. (14) are expressed as:

Table 4
main design parameters of the three heat exchangers.

High-Temperature Heat Exchanger (HT-HX)	
Heat transfer area	10.6 m^2
Reference length	2.36 mm
Flow area	17.9 cm^2
Inlet CO_2 temperature T_2	108.2 °C
Heat Recovery Vapor Generator (HRVG)	
Heat transfer area	3.62 m^2
Reference length	13.15 mm
Flow area	3.4 cm^2
R1233zDe evaporating pressure	35.6 bar
CO_2 gas cooler	
Heat transfer area	17.9 m^2
Reference length	2.36 mm
Flow area	22.03 cm^2
Cooling air-inlet temperature	25 °C
Cooling air pressure	1 bar
Cooling air mass flow rate	150 g/s

$$\begin{cases} \mathrm{Co} = \left(\dfrac{1-x}{x}\right)^{0.8}\left(\dfrac{\rho_{sv}}{\rho_{sl}}\right)^{0.5} \\ \mathrm{Bo} = \dfrac{P_{th}/A_{flow}}{m(h_{sv}-h_{sl})} \end{cases} \tag{16}$$

Inside the heat exchangers where the supercritical CO_2 is heated or cooled, the Dittus-Boelter correlations have been used (eq. (15)), where the Prandtl coefficient n is equal to 0.4 during heating and 0.3 during cooling.

The main specifics of the three heat exchangers designed according to engine operation point #4 are presented in Table 4. These data have been used for the off-design analysis of heat exchangers when they are crossed by the different exhaust gas flow rates of the other engine operating points (Table 3). Among those considered, this design point has been chosen for the engine owing to its average operating values; shifting the design point will only slightly affect the off-design performance on a single working point but not the overall behaviour. Different inlet temperatures were also considered.

3. Results and discussion

The model presented was preliminarily used to optimise the working conditions of the combined system.

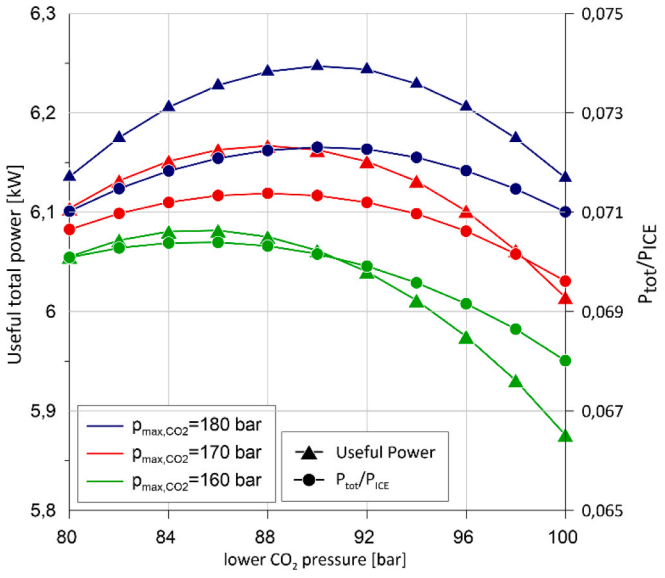

Fig. 9. total useful power produced by the combined system, varying the two pressure levels of the CO_2 Brayton cycle.

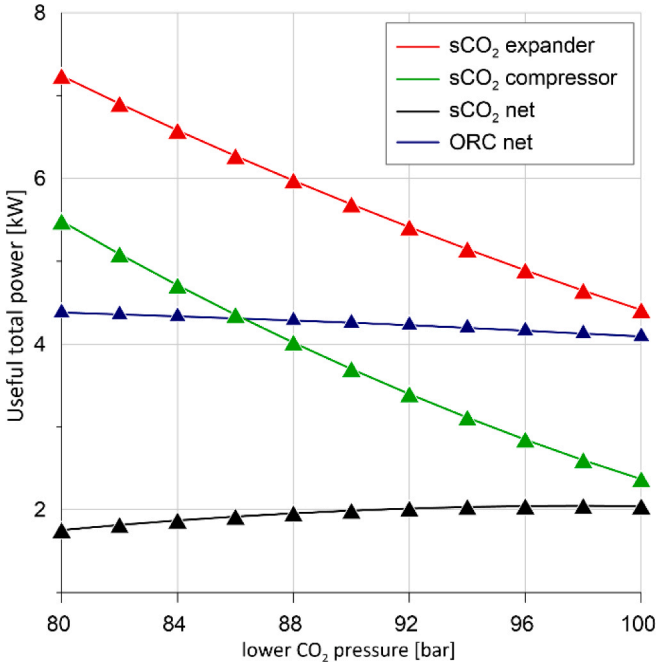

Fig. 10. Power produced by different sections of the combined recovery unit, varying the low sCO_2 pressure level ($p_{max,CO2}$ = 180 bar).

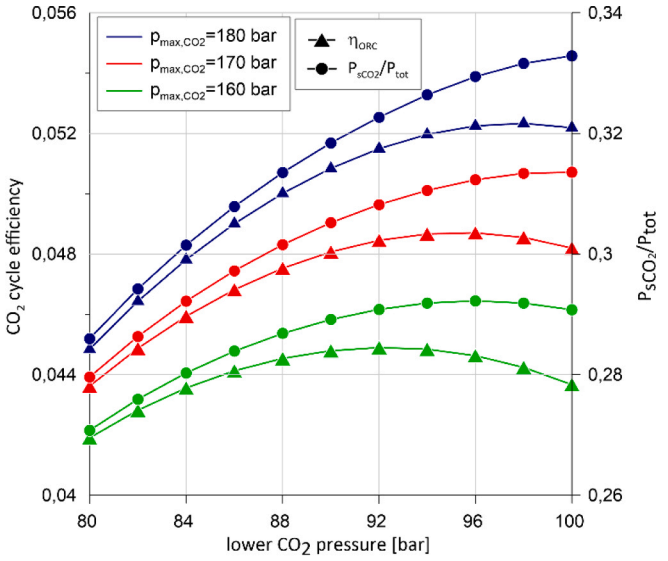

Fig. 11. sCO2 efficiency and repartition of supercritical CO2 power produced.

In particular, the two pressure levels of the CO_2 section have been varied and the results are shown in Figs. 9, 10 and 11. As expected, the higher the top pressure of the CO_2, the higher the total useful power produced by the system, as well as the ratio between the total power and that of the ICE. This is also true if the value of the produced power is divided per ICE mechanical power. A very interesting result is the possibility of finding the maximum value of the useful power as a function of the lower CO_2 pressure. For instance, a maximum recoverable power was obtained for a pressure equal to 88 bar when the top pressure was 170 bar; however, if the maximum CO_2 pressure was 180 bar, the maximum recoverable power was obtained for a lower pressure, equal to 90 bar. Hence, these values were chosen as the optimized pressure levels of the sCO_2 cycle. The influence of the lower CO_2 pressure is explained by Fig. 9 and Fig. 10: for a fixed $p_{max,CO2}$, when $p_{min,CO2}$ increases, the pressure ratio is reduced and, so, sCO_2 expander power decreases as well

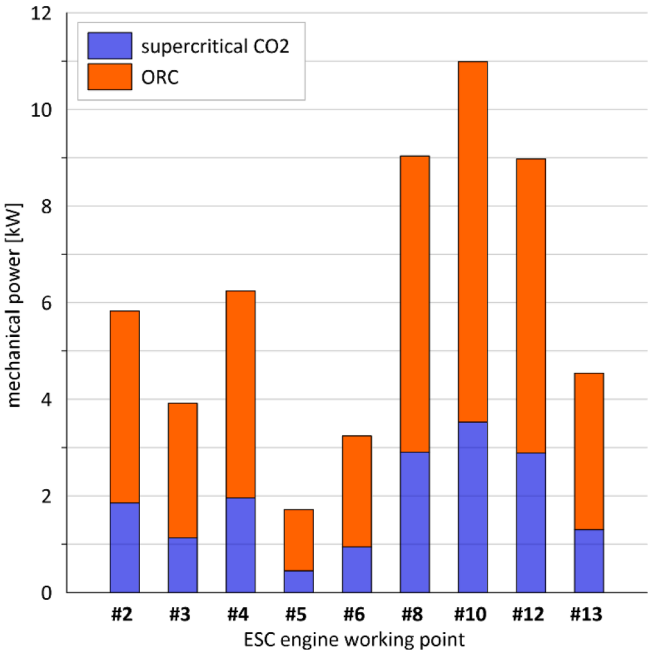

Fig. 12. Mechanical power produced by the combined recovery system in the different engine working points and its repartition between the two sections.

as the compressor power (red and green line of Figure 10); the net result is a slight increase of the mechanical power (black line of Fig. 10) and the increase in sCO_2 efficiency (Fig. 11). This is mainly related to the inlet density of the CO_2 at compressor, since lower temperature is fixed to 50 °C (linked to the availability of the cold sink on-board, i.e. environmental air). Therefore, the higher CO_2 cycle efficiency produces a lower thermal power available for the second recovery section, i.e. ORC section: lower organic fluid mass flow rate can be vaporized and, definitively, lower ORC mechanical power produced (Fig. 10).

A maximum value can also be obtained for the cycle efficiency of the carbon dioxide section, as demonstrated in Fig. 11; this also led to an increase in the importance of the CO_2 section with respect to the entire recovery system (dots and right axis of Fig. 11).

The optimized pressure levels have been used to evaluate the performances of the combined recovery unit for the overall ESC13 working points of the engine. The sCO_2 cycle operates between 90 and 180 bar (Fig. 8), with a maximum temperature fixed at 400 °C if the hot-side temperature difference is greater than 40 °C; the ORC cycle operates between 2.9 bar and 35.6 bar, with a maximum temperature fixed at 180 °C, to avoid fluid degradation. The bottom cycle is optimized according to the procedure described in [50]. The mechanical power recovered by the system is reported in Fig. 12, where the repartition between the two sections of the system has been highlighted. The ORC section is always the major component of the recovered mechanical power but the sCO_2 cycle always contributes significantly: it ranges from 26% to 32% of the mechanical recovered power, with higher values obtained with high exhaust gas temperatures downstream of the aftertreatment devices (ESC#8, #10, #12). ESC#4 can be individuated as the average working condition for the combined recovery system and is used as a reference working point for the off-design analysis.

Having fixed the thermodynamic characteristics of the ORC cycle, it remains unchanged for the overall ESC13 working points, with 52.44 °C at the pump exit (T_6) and 97.13 °C at the expander exit (T_8). On the contrary, even if the pressure levels of the sCO_2 cycle have been fixed, the temperatures at the expander inlet and outlet vary for each ESC13 working point due to different values of the exhaust temperature downstream of the aftertreatment devices. In Table 5, all the results for the ESC engine working points are presented in terms of thermodynamic data of the topping sCO_2 cycle. The significant variation in the exhaust gas thermal conditions causes variations in the sCO_2 cycle. It can be observed that in the highest engine working points (ESC#8, #10, #12), the maximum CO_2 temperature is reached (400 °C) and the thermodynamic cycle is the same. Conversely, in the ORC side, the maximum recoverable power condition is always reached and the thermodynamic cycle is the same for each ESC engine working point. The differences in recovered mechanical power are only related to mass flow rate variations, both in the sCO_2 and ORC sides, which in turn depends on the thermal power available in the exhaust gases.

Observing the working points studied, ESC #5 is that with the lowest recovery; this is due to the lower temperature of the exhaust gases, as confirmed by Fig. 13a, which plots the T-s diagrams of the three fluids (having ORC fluid entropy as reference). Fig. 13b shows the same

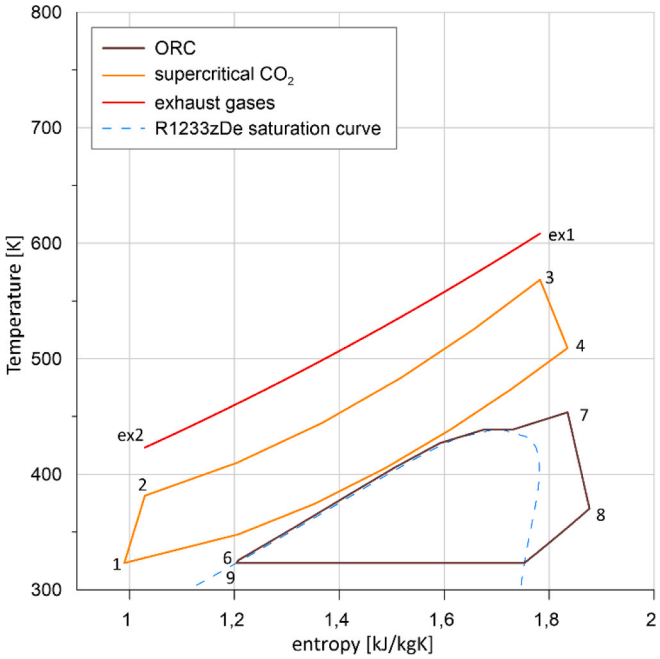

Fig. 13a. T-s diagram of the combined cycle in ESC #5 engine working point.

Table 5
results of the topping sCO_2 cycle.

ESC#	2	3	4	5	6	8	10	12	13
sCO_2 mass flow rate [kg/s]	0.0937	0.0840	0.1048	0.0498	0.0680	0.1405	0.1708	0.1395	0.0999
ORC mass flow rate [kg/s]	0.1264	0.0886	0.1363	0.0402	0.0731	0.1951	0.2373	0.1938	0.1031
T_1 [°C]	50	50	50	50	50	50	50	50	50
p_1 [bar]	88	88	88	88	88	88	88	88	88
T_2 [°C]	108.28	108.28	108.28	108.28	108.28	108.28	108.28	108.28	108.28
p_2 [bar]	180	180	180	180	180	180	180	180	180
T_3 [°C]	391.65	334.13	381.49	295.24	337.64	400.00	400.00	400.00	330.01
T_4 [°C]	329.63	273.96	319.82	236.10	277.37	337.69	337.69	337.69	269.95
T_5 [°C]	59.69	64.47	60.05	74.82	63.92	59.39	59.39	59.39	65.09

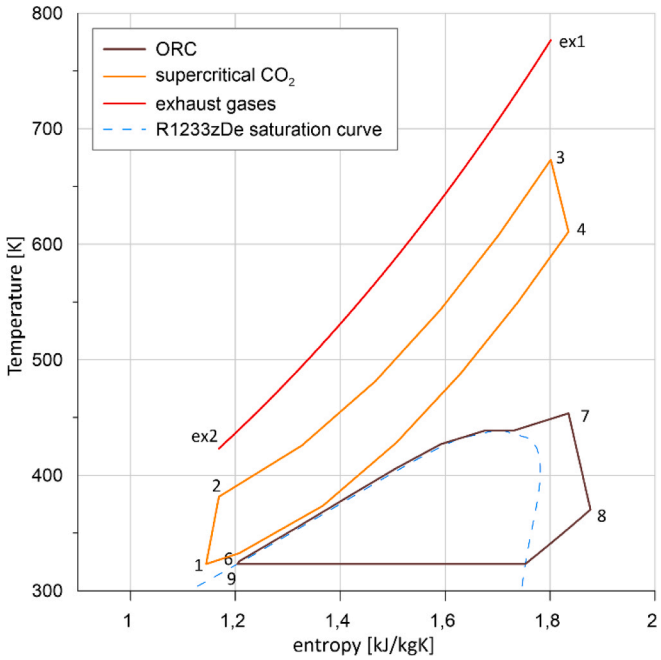

Fig. 13b. T-s diagram of the combined cycle in ESC #10 engine working point.

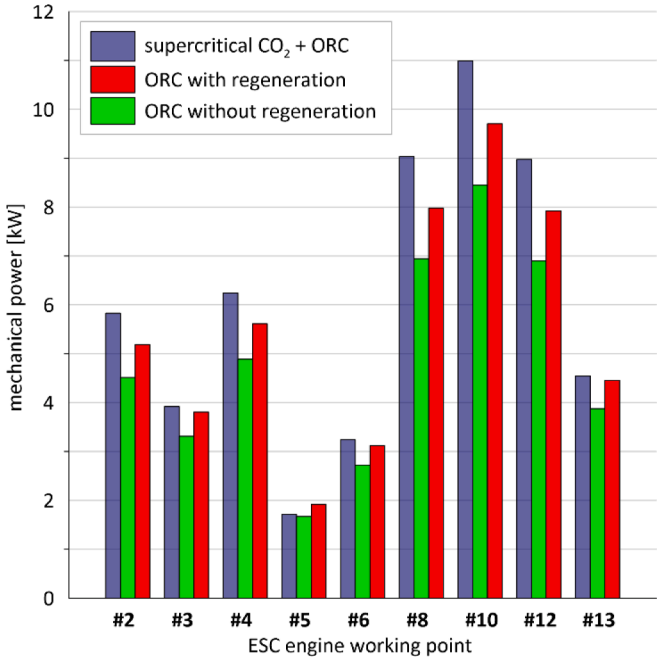

Fig. 14a. Comparison of mechanical power recovered among different systems.

entropy diagram for ESC#10, where the thermal energy available from the exhaust gases is highest. Comparing the two diagrams of Fig. 13, it is evident that the thermodynamic cycle of the ORC is the same (only the mass flow rate is changed) and the sCO_2 cycle fills the gap between the hot thermal source and ORC. It is also evident that the pinch point is moved inside the heat exchanger, which guarantees heating the organic fluid from the centre of the heat exchanger (Fig. 13a) to its inlet section from the organic fluid side.

The proposed combined system has also been compared to two different recovery systems: a single ORC with and without regeneration (Fig. 14), which is definitively more conventional. It has already been observed that, in the combined system, the sCO_2 regeneration stage is

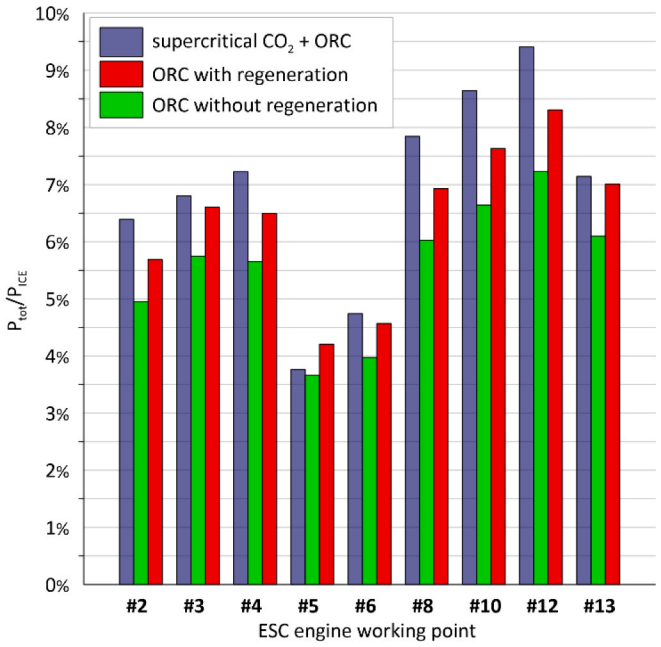

Fig. 14b. Comparison of mechanical power recovered among different systems in per cent of the ICE power.

unsuitable because the recovered thermal power from the exhaust gases would be reduced and the net useful power will be the same. Considering the combined system:

- regeneration in the ORC cycle would allow for an increased ORC mass flow rate, with a corresponding reduced heat recovery, approximately maintaining the mechanical power produced by the ORC cycle.
- regeneration in the sCO_2 cycle would reduce the heat recovery from the flue gases: it allows for increasing the CO_2 mass flow rate and the mechanical power produced by the sCO_2 cycle but drastically diminishes the heat recovery through the ORC cycle, with a significant reduction in the mechanical power produced by the combined system. The regeneration stage, in this case, could also be responsible for a significant share of exergy losses [59]. Moreover, the final exhaust gas exit temperature would be too high, reducing the engine operating points suitable for recovery.

Except for case ESC#5, the combined system always has a higher recovered mechanical power. On average, 1% more ICE power is produced in the ESC13 modes.

The mechanical power produced by the combined system is in the range of 2 kW (ESC#5) and 11 kW (ESC#10), which is a significant value for the considered engine. Referring the produced power to the brake power of the engine, these values account for 4 – 9% of the ICE power. The sole ORC produces approximately 8.5 kW (7% of the ICE power) in the best case (ESC#10); when it is regenerated, for the same engine working point, the recovered mechanical power increases to 9.6 kW (8.3% of the ICE power). The additional power produced by the sCO_2 cycle is up to 30% more than sole ORC and is, on average, 23% higher. For the lowest engine load working point (ESC#5), the situation is reversed; this is the only working point where the regenerated ORC unit has a recovered mechanical power higher than that for the combined cycle. In reality, the power produced by the sCO_2/ORC and the sole ORC are quite similar (1.9 kW) but is slightly higher when the regeneration stage is considered in the sole ORC (approximately 2 kW, Fig. 14a); this is because of the low CO_2 mass flow rate and the consequent very low contribution of the sCO_2 in this low-load engine working point (Fig. 12 and Table 5).

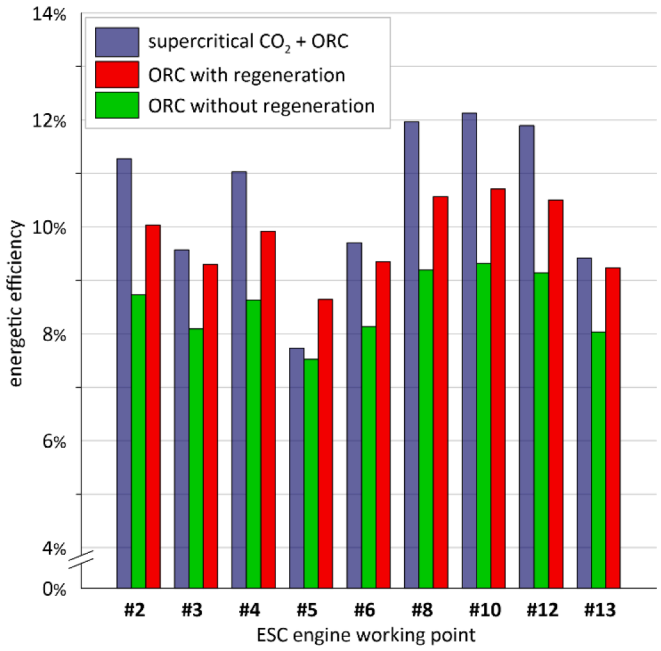

Fig. 15a. Comparison between different recovery systems in terms of energetic efficiency.

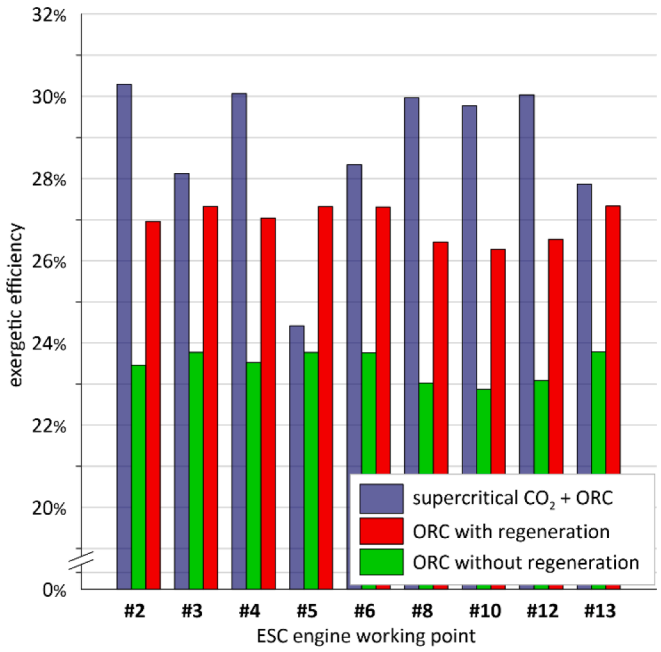

Fig. 15b. Comparison between different recovery systems in terms of exergetic efficiency.

The introduction of the supercritical CO_2 cycle between the exhaust gases and the ORC unit increases the energy efficiency of the system (Fig. 15a) since higher mechanical power is produced for the same thermal power available at the exhaust. More importantly, the exergetic efficiency improves, which is up to 7 percentage points higher owing to the CO_2 supercritical cycle (Fig. 15b). In particular, energetic efficiency is interesting, being in the range of 7 – 12 % while the sole ORC does not reach 10% and overcomes this value only for some engine working points, owing to a regeneration stage (Fig. 15a). Even more interesting is the exergetic efficiency; the good agreement between the thermal curves results in a very high value (above 30% in many engine working points) while the sole ORC cannot overcome 24% and, in the best cases, reaches 27% with regeneration (Fig. 15b). As shown, higher exergetic efficiency values with the combined sCO_2 and ORC cycle were obtained for engine working points with exhaust gas temperatures higher than 420 °C (ESC#2, #4, #8, #10, #12). In these cases, as shown in Fig. 13b, the sCO_2 topping cycle exploits the considerable thermodynamic room present between the exhaust gas cooling and the preheating-vaporizing-superheating in the ORC cycle and allows a drastic reduction in exergy losses due to the heat transfer with temperature differences.

The exergetic flows are summarized in the Grassmann diagram of Fig. 16, where the exergy of the exhaust gases is reduced by the irreversibilities introduced in each component. In the same figure, the contribution to the exergy flows of the two main recovery sections, sCO_2 and ORC, can be recognized. If only the sCO_2 section is considered, the heat reversed to the cold sink would be completely wasted, representing a huge exergy loss. The main exergy losses are related to the gases at the stack and heat exchange section. When compared to a single ORC unit (Fig. 17), the exergy loss related to the HRVG is by far the most important and, thus, the one that is mostly reduced by the combined system; this is due to the high average temperature difference between the two fluids, which justifies the introduction of an intermediate cycle, maintaining the ORC characteristics.

The performances reported in Figs. 14a, 14b, 15a and 15b are the results of Eq. (3) and Eq. (7), expressing the two mechanical powers, and of Eq. (8) and Eq. (10) concerning the two efficiencies. Exergy flows were calculated according to Eq. (9). Each engine operating point corresponds to different designs for the three heat exchangers.

A more engineering-based analysis was performed by choosing an engine operating point (#4), designing the three heat exchangers according to Eqs. (12) – (16) (Table 3) and performing an off-design study, observing the performances of the combined recovery unit when the engine operating point changes (mass flow rate of the exhaust gas and temperature). The intention is to evaluate the performance of a pre-designed combined unit when the heat source changes according to the most relevant engine operating conditions.

Fig. 18 shows the thermal power exchanged in the considered engine working points. The results showed that the designed heat exchangers (HT-HX, HRVG, and CO_2 cooler) can satisfy the thermal power to be exchanged.

This is also verified for the outlet temperatures, as shown in Fig. 19. The following considerations apply:

The temperature of the CO_2 at the compressor inlet (T_1) is very close to the target temperature (50 °C), demonstrating the good behaviour of the CO_2 cooler (red bars in Fig. 19). This guarantees a low power absorbed by the compressor.

The temperature of the organic working fluid at the HRVG exit (T_7) is always very close to the target value (180 °C), demonstrating the good behaviour of the heat exchanger in off-design conditions and guarantees correct superheating of the fluid at the ORC expander inlet.

The temperature of the exhaust gases leaving HT-HX (T_{ex2}) is targeted at 150 °C but its final value is often approximately 135 – 140 °C. The difference with respect to the target value is acceptable and a lower temperature of the gases corresponds to a higher heat value exchanged in the HT-HX, increasing the recovered thermal power.

The maximum temperature of the CO_2 (T_3) is strictly dependent on the engine working point: its target (yellow dashed line in Fig. 19) is between 300 °C and 400 °C and the resulting temperature follows the target with little deviation (less than 15 °C).

4. Conclusions

Waste heat recovery and conversion into mechanical energy is one of the most promising opportunities to reduce fuel consumption in internal combustion engines. The most referenced technology is related to the use of an organic fluid to perform a Rankine or superheated (Hirn) thermodynamic cycle. The low efficiency of these cycles when they are

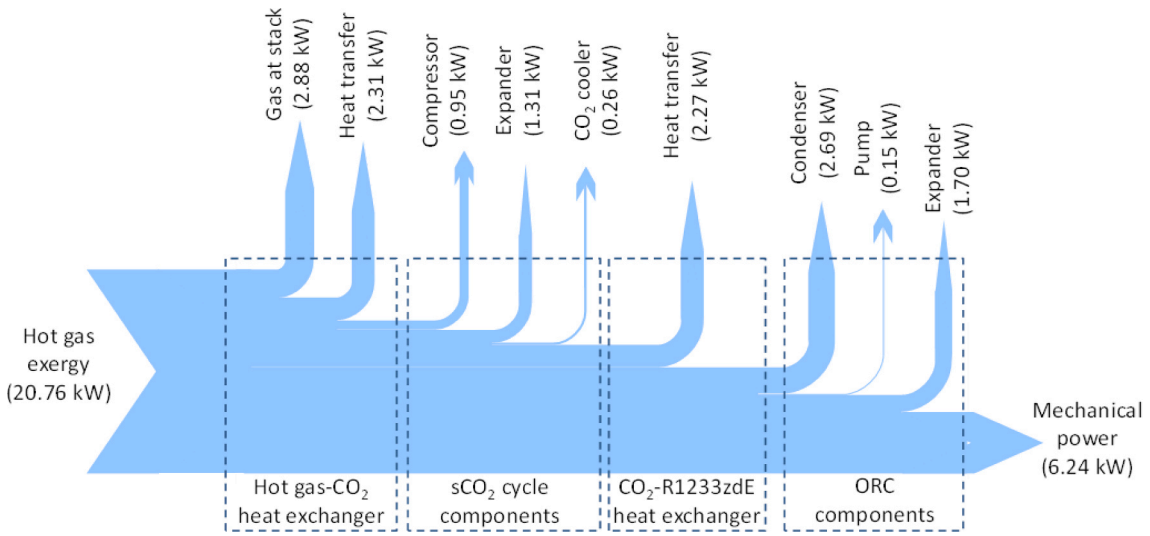

Fig. 16. Grassmann diagram of exergetic flows for combined supercritical CO_2 and ORC recovery system bottoming an internal combustion engine performing ESC #4 working point.

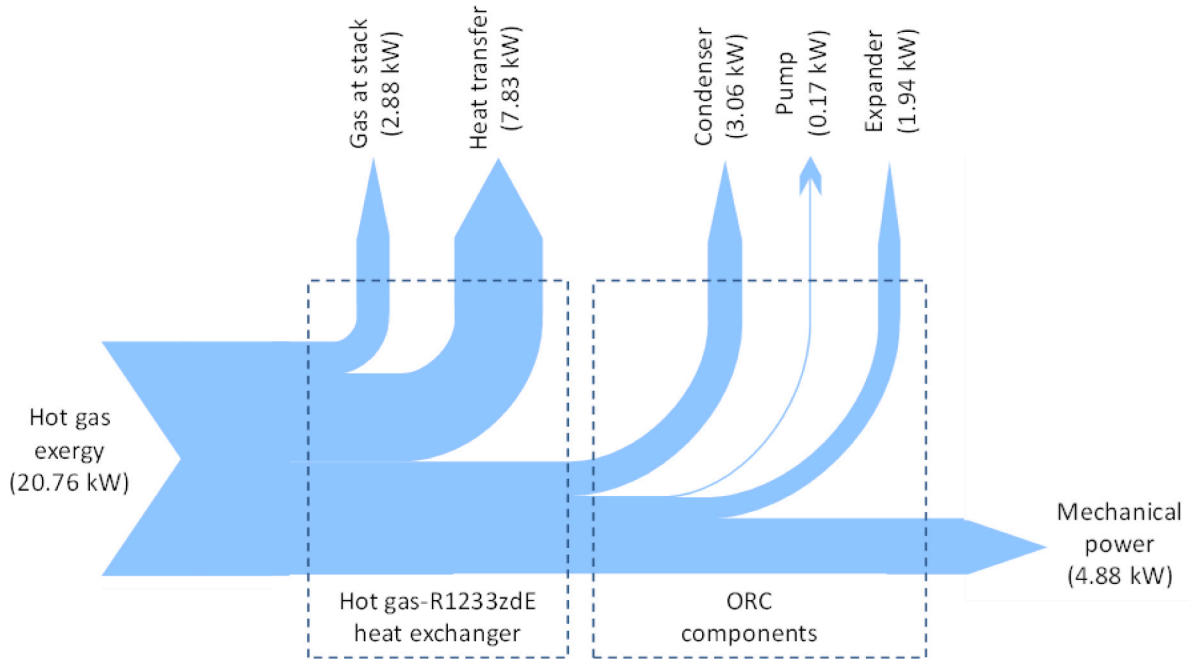

Fig. 17. Grassmann diagram of exergetic flows for an ORC recovery system bottoming an internal combustion engine performing ESC #4 working point.

fed by a heat source representative of the ICE exhaust gases and the further reduction when the real efficiencies of the machines are introduced call for further thermodynamic and technological efforts. Therefore, a combined recovery cycle has been proposed, comprising a supercritical CO_2 Brayton cycle and a cascade ORC section that utilizes R1233zDe as the working fluid.

The heat source was experimentally characterized considering a turbocharged 3L diesel engine (IVECO F1C used both as light and heavy-duty applications) for the 13 points specified by the ESC-13 mode experimental procedure. Assumptions have been made to keep the results close to the real operation:

(a) a suitable maximum temperature of the supercritical CO_2 not above 400 °C;
(b) full vaporisation of the organic fluid, reaching a maximum temperature of 180 °C
(c) suitable cooling of the CO_2 at the compressor inlet, with a temperature equal to 50 °C.

The mechanical power recovered is up to 9% of the brake power of the engine, considering the actual performance of the ORC-based power units, measured with a heat sink temperature equal to 40 °C (real on-board conditions for external air). The same figure (9%) applies to CO_2 reduction.

Efficiencies (both of first and second thermodynamic laws) are significantly higher when the combined plant is considered: 3 – 4% points of efficiency can be gained with this system compared to the more conventional ORC-based power unit only. Indeed, the major source of irreversibility (i.e., the high-temperature heat exchanger) reduces its importance owing to the much closer thermal exchange curves (T-s plan) and the small pinch temperature difference achieved.

A very important result has been achieved by performing an off-

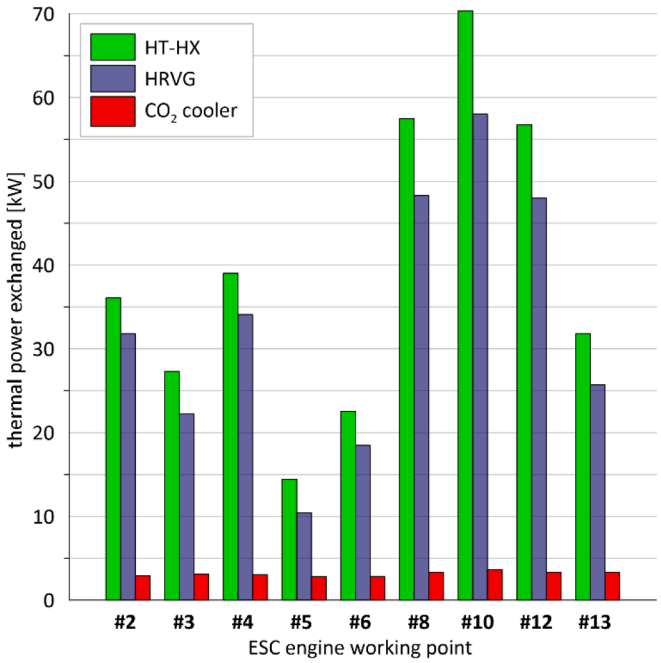

Fig. 18. Off-design resulted in heat exchanged in the three heat exchangers for the different engine working points considered.

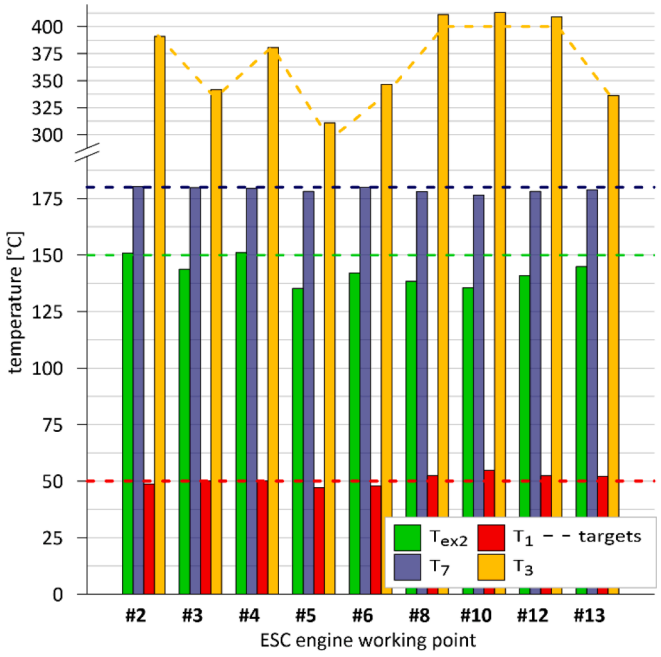

Fig. 19. Off-design resulted in outlet temperatures in the three heat exchangers for the different engine working points considered.

design analysis that represents how a given design of the combined unit would behave when the engine is operated at different operating points. This analysis is mandatory as ICE equipping long-haul vehicle operates in off-design conditions, arranging the engine load and speed to the required mechanical power. Hence, the three major heat exchangers in the combined unit have been designed and sized for a suitable ICE working point (among those experimentally available). Their correct behaviour has been verified by observing that when the engine runs all the ESC13-modes, the three conditions that make the operation of the combined unit possible (a suitable maximum temperature of supercritical CO_2, full vaporisation of the organic fluid, and suitable cooling of the CO_2 at the compressor inlet) are safely guaranteed.

Even though an economic analysis is beyond the scope of this paper, a final remark is considered useful and could invite further specific investigations. For ORC-based power, unit costs referenced in the literature can be considered and introduced in a cost-benefit analysis [60]; unfortunately, the same information is unavailable for the sCO_2-based power unit, although some estimations could be made. Much more difficult is the evaluation of the benefits; on board of vehicles, energy recovery is certainly useful and is immediately reflected in fuel-cost saving; however, the most important benefit is the reduction of CO_2. Its economic benefit must be accounted for, but is difficult to estimate, particularly in the transportation sector.

CRediT authorship contribution statement

D. Di Battista: Data curation, Investigation, Methodology, Validation, Visualization, Writing - original draft. **F. Fatigati:** Data curation, Investigation, Software, Validation, Writing - original draft. **R. Carapellucci:** Conceptualization, Data curation, Formal Analysis, Investigation, Software, Supervision, Writing - review and editing. **R. Cipollone:** Conceptualization, Formal analysis, Funding acquisition, Methodology, Resources, Supervision, Writing - review and editing.

Declaration of Competing Interest

The authors declare that they have no known competing financial interests or personal relationships that could have appeared to influence the work reported in this paper.

Acknowledgments

This paper has been written in the time framework of the EU project LONGRUN – Development of an efficient and environmentally friendly LONG distance powertrain for heavy-duty trucks and coaches. Also the Project “Hyper – Hybrid Propulsion for Electric Realignment” – POR FESR 2014-2020 – Call HUB Ricerca e Innovazione is acknowledged.

References

[1] Anton Firth, Bo Zhang, Aidong Yang, Quantification of global waste heat and its environmental effects, Applied Energy, Volume 235, 2019, Pages 1314-1334, ISSN 0306-2619, https://doi.org/10.1016/j.apenergy.2018.10.102.
[2] Lahoud C, Al Asmar J, Brouche M. Review of cogeneration and trigeneration systems. Afr J Eng Res 2018;6(3):39–54.
[3] Zirngibl, S.A., Günter, F., Prager, M., Wachtmeister, G., Simulative Evaluation of Various Thermodynamic Cycles and the Specification of Their System Components Regarding the Optimization of a Cogeneration Unit, (2017) SAE Technical Papers.
[4] Semmari, H., Filali, A., Aberkane, S., Feidt, R., Feidt, M., Flare gas waste heat recovery: Assessment of organic rankine cycle for electricity production and possible coupling with absorption chiller, (2020) Energies, 13 (9), art. no. 2265.
[5] Pan, Q., Peng, J., Wang, R., Experimental study of an adsorption chiller for extra low temperature waste heat utilization, (2019) Applied Thermal Engineering, 163, art. no. 114341.
[6] Borri E, Tafone A, Comodi G, Romagnoli A. Improving liquefaction process of microgrid scale Liquid Air Energy Storage (LAES) through waste heat recovery (WHR) and absorption chiller. Energy Proc 2017;143:699–704.
[7] Nami H, Arabkoohsar A. Improving the power share of waste-driven CHP plants via parallelization with a small-scale Rankine cycle, a thermodynamic analysis. Energy 2019;171:27–36.
[8] Cipollone R, Di Battista D, Bettoja F. Performances of an ORC power unit for waste heat recovery on heavy duty engine. Energy Proc 2017;129:770–7.
[9] Pili R, Romagnoli A, Spliethoff H, Wieland C. Techno-economic analysis of waste heat recovery with orc from fluctuating industrial sources. Energy Proc*** 2017; 129:503–10.
[10] Di Battista, D., Di Bartolomeo, M., Villante, C., Cipollone, R., A Model Approach to the Sizing of an ORC Unit for WHR in Transportation Sector, (2017) SAE International Journal of Commercial Vehicles, 10 (2).
[11] Rattner AS, Meehan TJ. Simple analytic model for optimally sizing thermoelectric generator module arrays for waste heat recovery. Appl Therm Eng 2019;146: 795–804.
[12] Di Battista, D., Carapellucci, R., Cipollone, R., Integrated evaluation of Inverted Brayton cycle recovery unit bottomed to a turbocharged diesel engine, (2020)

Applied Thermal Engineering, 175, art. no. 115353. doi:10.1016/j.applthermaleng.2020.115353.
[13] Arminio, F., Cameretti, M., De Simio, L., Iannaccone, S. et al., "Modeling of a Spark Ignition Engine with Turbo-Generator for Energy Recovery," SAE Technical Paper 2019-24-0084, 2019, https://doi /10.4271/2019-24-0084.
[14] Di Battista D, Cipollone R. Experimental analysis of an organic rankine cycle plant bottoming a heavy-duty engine using axial turbine as prime mover. SAE Int. J. Engines 2017;10(4):1385–97. https://doi/10.4271/2017-01-9279.
[15] Cipollone, R., Bianchi, G., Gualtieri, A., Di Battista, D., Mauriello, M., Fatigati, F., Development of an Organic Rankine Cycle system for exhaust energy recovery in internal combustion engines, (2015) Journal of Physics: Conference Series, 655 (1), art. no. 012015.
[16] Yang Y, Zhang H, Xu Y, Zhao R, Hou X, Liu Y. Experimental study and performance analysis of a hydraulic diaphragm metering pump used in organic Rankine cycle system. Appl Therm Eng 2018;132:605–12.
[17] Yang Y, Zhang H, Tian G, Xu Y, Wang C, Gao J. Performance analysis of a multistage centrifugal pump used in an Organic Rankine Cycle (ORC) system under various condensation conditions. J Therm Sci 2019;28(4):621–34.
[18] Zhu YD, Jiang L, Zhou YD, Yu LJ. An integrated comparison for working fluids selection in both subcritical and supercritical ORC. Adv Mater Res 2014;997:703–12.
[19] Kizilkan O. Performance assessment of steam Rankine cycle and sCO2 Brayton cycle for waste heat recovery in a cement plant: a comparative study for supercritical fluids. Int J Energy Res. 2020.
[20] Antti Uusitalo, Alireza Ameli, Teemu Turunen-Saaresti, Thermodynamic and turbomachinery design analysis of supercritical Brayton cycles for exhaust gas heat recovery, Energy, Volume 167, 2019, Pages 60-79, ISSN 0360-5442, https://doi.org/10.1016/j.energy.2018.10.181.
[21] Chen H, Goswami DY, Stefanakos EK. A review of thermodynamic cycles and working fluids for the conversion of low-grade heat. Renew Sustain Energy Rev 2010;14(9):3059–67.
[22] Danieli P, Rech S, Lazzaretto A. Supercritical CO2 and air Brayton-Joule versus ORC systems for heat recovery from glass furnaces: performance and economic evaluation. Energy 2019;168:295–309.
[23] Astolfi M, Alfani D, Lasala S, Macchi E. Comparison between ORC and CO2 power systems for the exploitation of low-medium temperature heat sources. Energy 2018;161:1250–61.
[24] Akbari AD, Mahmoudi SMS. Thermoeconomic analysis and optimization of the combined supercritical CO2 (carbon dioxide) recompression Brayton/organic Rankine cycle. Energy 2014;78:501–12.
[25] Ren, L., Wang, H., Optimization and comparison of two combined cycles consisting of CO2 and organic trans-critical cycle for waste heat recovery, (2020) Energies, 13 (3), art. no. 724.
[26] Francesco Crespi, Giacomo Gavagnin, David Sánchez, Gonzalo S. Martínez, Supercritical carbon dioxide cycles for power generation: A review, Applied Energy, Volume 195, 2017, Pages 152-183, ISSN 0306-2619, https://doi.org/10.1016/j.apenergy.2017.02.048.
[27] Hou S, Zhou Y, Yu L, Zhang F, Cao S. Optimization of the combined supercritical CO2 cycle and organic, Rankine cycle using zeotropic mixtures for gas turbine waste heat recovery. Energy Convers. Manage. 2018;160:313–25.
[28] Manente, G., Fortuna, F.M., Supercritical CO2 power cycles for waste heat recovery: A systematic comparison between traditional and novel layouts with dual expansion, (2019) Energy Conversion and Management, 197, art. no. 111777.
[29] Kolasinski, P., The method of the working fluid selection for organic Rankine cycle (ORC) systems employing volumetric expanders, (2020) Energies, 13 (3), art. no. 573.
[30] Klimaszewski P, Zaniewski D, Witanowski Ł, Suchocki T, Klonowicz P, Lampart P. A case study of working fluid selection for a small-scale waste heat recovery ORC system. Archiv Thermodyn 2019;40(3):158–80.
[31] Zhao M, Wei M, Song P, Liu Z, Wang Z. Effects of the ORC operating conditions on the engine performance for an engine-ORC combined system. Energy Proc 2017;105:662–7.
[32] Yang K, Zhang H, Song S, Yang F, Liu H, Zhao G, et al. Effects of degree of superheat on the running performance of an organic rankine cycle (ORC) waste heat recovery system for diesel engines under various operating conditions. Energies 2014;7(4):2123–45.
[33] Macchi, E., Astolfi, M., Organic Rankine Cycle (ORC) Power Systems: Technologies and Applications, (2016) Organic Rankine Cycle (ORC) Power Systems: Technologies and Applications, pp. 1-679.
[34] Di Battista, D., Mauriello, M., Cipollone, R., Effects of an ORC Based Heat Recovery System on the Performances of a Diesel Engine, (2015) SAE Technical Papers, 2015-April (April).
[35] Zhao M, Wei M, Song P, Liu Z, Tian G. Performance evaluation of a diesel engine integrated with ORC system. Appl. Therm Eng 2017;115:221–8.
[36] Wu, X., Chen, J., Xie, L., Optimal design of organic Rankine cycles for exhaust heat recovery from light-duty vehicles in view of various exhaust gas conditions and negative aspects of mobile vehicles, (2020) Applied Thermal Engineering, 179, art. no. 115645.
[37] Usman M, Imran M, Yang Y, Park B-S. Impact of organic Rankine cycle system installation on light duty vehicle considering both positive and negative aspects. Energy Convers Manage 2016;112:382–94.
[38] Seitz, D., Gehring, O., Bunz, C., Brunschier, M., Sawodny, O., Design of a Nonlinear, Dynamic Feedforward Part for the Evaporator Control of an Organic Rankine Cycle in Heavy Duty Vehicles, (2016) IFAC-PapersOnLine, 49 (11), pp. 625-632.
[39] Imran M, Park B-S, Kim H-J, Lee D-H, Usman M. Economic assessment of greenhouse gas reduction through low-grade waste heat recovery using organic Rankine cycle (ORC). J Mech Sci Technol 2015;29(2):835–43.
[40] Tocci, L., Toro, C., Thermo-economic comparison of single and dual loop ORC for industrial waste heat recovery, (2017) 30th International Conference on Efficiency, Cost, Optimization, Simulation and Environmental Impact of Energy Systems, ECOS 2017.
[41] Persyn, D., Díaz-Lanchas, J., Barbero, J., Estimating road transport costs between EU regions JRC Working Papers on Territorial Modelling and Analysis No 04/2019.
[42] ACEA Paper: CO2 emissions from heavy-duty vehicles – Preliminary CO2 baseline (Q3-Q4 2019), March 2020.
[43] ICCT - CO2 STANDARDS FOR HEAVY-DUTY VEHICLES IN THE EUROPEAN UNION, April 2019.
[44] Yang J, Ye Z, Yu B, Ouyang H, Chen J. Simultaneous experimental comparison of low-GWP refrigerants as drop-in replacements to R245fa for Organic Rankine cycle application: R1234ze(Z), R1233zd(E), and R1336mzz(E). Energy 2019;173:721–31.
[45] Guillaume L, Legros A, Desideri A, Lemort V. Performance of a radial-inflow turbine integrated in an ORC system and designed for a WHR on truck application: an experimental comparison between R245fa and R1233zd. Appl Energy 2017;186:408–22.
[46] Fatigati, F., Di Bartolomeo, M., Di Battista, D., Cipollone, R., Experimental and numerical characterization of the sliding rotary vane expander intake pressure in order to develop a novel control-diagnostic procedure, (2019) Energies, 12 (10), art. no. 1970.
[47] Fatigati, F., Di Bartolomeo, M., Di Battista, D., Cipollone, R., Experimental characterization of a hermetic scroll expander operating in an ORC-based power unit bottoming an internal combustion engine, (2019) AIP Conference Proceedings, 2191, art. no. 020069.
[48] Bianchi G, Fatigati F, Murgia S, Cipollone R. Design and analysis of a sliding vane pump for waste heat to power conversion systems using organic fluids. Appl Therm Eng 2017;124:1038–48.
[49] Olmedo LE, Mounier V, Mendoza LC, Schiffmann J. Dimensionless correlations and performance maps of scroll expanders for micro-scale Organic Rankine Cycles. Energy 2018;156:520–33.
[50] Di Battista D, Cipollone R, Villante C, Fornari C, Mauriello M. The potential of mixtures of pure fluids in ORC-based power units fed by exhaust gases in internal combustion engines. Energy Proc 2016;101:1264–71.
[51] Kim, Sarah; Rached, Wissam; and Abbas, Laurent, "Performance and Stability of E-1233zd in Energy Recovery Applications" (2018). International Refrigeration and Air Conditioning Conference. Paper 2053.
[52] Marchionni M, Bianchi G, Tassou SA. Techno-economic assessment of Joule-Brayton cycle architectures for heat to power conversion from high-grade heat sources using CO2 in the supercritical state. Energy 2018;148:1140–52.
[53] Santini, F., Di Battista, D., Villante, C., Orlandi, M., Transcritical CO2 refrigeration plants: Experimental campaign and model-based evaluations of new technologies, (2019) AIP Conference Proceedings, 2191, art. no. 020136.
[54] Bianchi G, Saravi SS, Loeb R, Tsamos KM, Marchionni M, Leroux A, et al. Design of a high-temperature heat to power conversion facility for testing supercritical CO2 equipment and packaged power units. Energy Proc 2019;161:421–8.
[55] Jian Song, Xiaoya Li, Kai Wang, Christos N. Markides, Parametric optimisation of a combined supercritical CO2 (S-CO2) cycle and organic Rankine cycle (ORC) system for internal combustion engine (ICE) waste-heat recovery, Energy Conversion and Management, Volume 218, 2020, 112999, ISSN 0196-8904.
[56] Fatigati, F., Di Bartolomeo, M., Di Battista, D., Cipollone, R., A dual-intake-port technology as a design option for a Sliding Vane Rotary Expander of small-scale ORC-based power units, (2020) Energy Conversion and Management, 209, art. no. 112646.
[57] Marchionni M, Chai L, Bianchi G, Tassou SA. Numerical modelling and performance maps of a printed circuit heat exchanger for use as recuperator in supercritical CO2 power cycles. Energy Proc 2019;161:472–9.
[58] Cipollone, R., Bianchi, G., Di Battista, D., Fatigati, F., Experimental and numerical analyses on a plate heat exchanger with phase change for waste heat recovery at off-design conditions, (2015) Journal of Physics: Conference Series, 655 (1), art. no. 012038.
[59] Mingzhang Pan, Yan Zhu, Xingyan Bian, Youcai Liang, Fulu Lu, Zhibo Ban, Theoretical analysis and comparison on supercritical CO2 based combined cycles for waste heat recovery of engine, Energy Conversion and Management, Volume 219, 2020, 113049, ISSN 0196-8904.
[60] Vittorini Diego, Roberto Carapellucci, Roberto Cipollone, Enhanced performances of ORC-based power units for low grade waste heat recovery via evaporator optimization, Energy Conversion and Management, Volume 197, 2019, 111874, ISSN 0196-8904.

Io sottoscritto Fabio Fatigati, co-autore dell'articolo scientifico: "An improvement to waste heat recovery in internal combustion engines via combined technologies" pubblicato sulla rivista internazionale Energy Conversion and Management, (https://doi.org/10.1016/j.enconman.2021.113880), dichiaro che i contributi degli autori nello sviluppo del presente articolo sono i seguenti:

- Davide Di Battista: Data curation, Investigation, Methodology, Validation, Visualization, Writing - original draft;
- **Fabio Fatigati**: Data curation, Investigation, Software, Validation, Writing - original draft;
- Roberto Carapellucci: Conceptualization, Data curation, Formal Analysis, Investigation, Software, Supervision, Writing - review and editing;
- Roberto Cipollone: Conceptualization, Formal analysis, Funding acquisition, Methodology, Resources, Supervision, Writing - review and editing.

L'indicazione sui contributi degli autori è riportata nel *CRediT authorship contribution statement* a pagina 13 del medesimo articolo.

In fede, L'Aquila 24/09/2021

Fabio Fatigati